Acta Cryst. (1978). B**34**, 3149–3156

Electron-Density Distribution in Crystals of α-K_2CrO_4

BY K. TORIUMI AND Y. SAITO

The Institute for Solid State Physics, The University of Tokyo, Roppongi-7, Minato-ku, Tokyo 106, *Japan*

(*Received* 17 *February* 1978; *accepted* 12 *May* 1978)

The electron-density distribution in crystals of α-K_2CrO_4 has been determined by single-crystal X-ray diffraction. The effective charges of the atoms were estimated by the direct integration of valence-electron density to be Cr +0·1 (1), O −0·5 (1), and K +1·0 (1) e. The largely neutralized charges of the Cr and O atoms indicate a significant contribution of the 3*d* atomic orbitals of the Cr atom to the Cr–O bonding orbitals. The residual electron density around the Cr atom was observed on the deformation map which was averaged by assuming T_d symmetry for the CrO_4^{2-} ion. The asphericity indicates an excess charge in the t_2 orbitals and a deficiency in the *e* orbitals. The residual peak attributed to the Cr–O bonding electrons shows π-bond character.

Introduction

In our series of studies on electron-density distributions in octahedral transition-metal complexes, an aspherical distribution of 3*d* electrons in non-bonding orbitals was directly observed by X-ray diffraction (Iwata & Saito, 1973; Marumo, Isobe, Saito, Yagi & Akimoto, 1974; Marumo, Isobe & Akimoto, 1977; Iwata, 1977). A similar asphericity was also observed in the vicinity of a transition-metal atom placed in a T_d environment (Toriumi, Ozima, Akaogi & Saito, 1978). However, no attempt has yet been made to observe an aspherical distribution of 3*d* electrons in a covalent cluster containing a transition-metal atom, where the 3*d* electrons contribute to bonding.

The study of the electron-density distribution in the CrO_4^{2-} ion, an oxo acid of a transition-metal, has been undertaken to observe the asphericity of the 3*d* electrons in bonding orbitals. The Cr atom has a marked tendency to form covalent bonds, because the high formal charge of +6 on the Cr atom in CrO_4^{2-} means strong polarization of the O atoms. Thus the electron-density distribution around the Cr atom has to be treated by a molecular-orbital method.

Experimental

Single crystals of α-K_2CrO_4 were grown by recrystallization of the commercial product from water. Weissenberg photographs were taken with Cu $K\alpha$ radiation to check the space group and the unit-cell dimensions already reported (Zachariasen & Ziegler, 1931; Pistorius, 1962). The values found agreed with those reported within experimental error.

The crystal specimen used for X-ray work was shaped into a sphere 0·16 mm in diameter by etching with a piece of wet filter paper. Unit-cell dimensions were refined by least-squares calculations on the basis of 20 2θ values ($24° \le 2\theta \le 44°$) measured on a diffractometer with Mo $K\alpha$ radiation.

The crystal data are: orthorhombic, *Pnma*, $Z = 4$, $a = 7{\cdot}662$ (1), $b = 5{\cdot}919$ (1), $c = 10{\cdot}391$ (1) Å, $U = 471{\cdot}2$ (1) Å^3, μ(Mo $K\alpha$) = 40·34 cm^{-1}, $D_x = 2{\cdot}74$ g cm^{-3}.

The intensity data were collected on a Rigaku automated four-circle diffractometer with Mo $K\alpha$ radiation monochromated by a graphite plate. The experimental conditions are broadly similar to those described by Iwata & Saito (1973) and listed in Table 1. 3949 reflexions with $h,k,l \ge 0$ were measured up to a 2θ value of 135°. In addition, 248 reflexions with $h,k,\bar{l} \ge 0$ within the range $0° < 2\theta \le 40°$ were measured in order to reduce the systematic errors in $|F_o|$. 3125 intensities with $|F_o| \ge 3\sigma(|F_o|)$ were collected; of these, 2890 were independent (hereafter data set 1).

Comparison of the observed intensities for symmetry-related reflexions, hkl and $hk\bar{l}$, indicated

Table 1. *Experimental conditions*

Diameter of the spherical specimen	0·16 mm
Radiation	Mo $K\alpha$ ($\lambda = 0{\cdot}71069$ Å)
Monochromator	Graphite plate (002)
Scan mode	θ–2θ continuous scan
Scan rate	2°(θ) min^{-1} ($2\theta \le 60°$)
	1°(θ) min^{-1} ($2\theta > 60°$)
Scan width	$1{\cdot}4° + 0{\cdot}8° \tan\theta$
Background counting time	15 ~ 340 s
Maximum number of repetitions	4
Criterion to terminate repetition	$\sigma(\|F\|)/\|F\| \le 0{\cdot}003$
$2\theta_{max}[(\sin\theta/\lambda)_{max}]$	135° [1·30 Å^{-1}]
Total number of measured reflexions	4195
Number of observed independent reflexions [$\|F\| \ge 3\sigma(\|F\|)$]	2890

significant differences in some strong low-angle reflexions. The differences appeared to be due to anisotropic extinction. Accordingly, the variations of the integrated intensities with azimuthal angle Ψ were measured for some strong low-angle reflexions. This measurement was carried out on an automated four-circle diffractometer with similar conditions to those given in Table 1. In order to check whether the crystal specimen was completely in the direct beam in all orientations, an image of the direct beam was recorded on an X-ray film. The intensities of 19 reflexions were measured at 10–30° intervals of Ψ within the range $0° \leq \Psi < 360°$ (except for the mechanically blind regions) (hereafter data set 2). The maximum intensity variation was as large as 5% in $|F_o|$ for the 002 reflexion.

The intensities were corrected for Lorentz and polarization factors. An absorption correction was also applied on the assumption that the specimen was a sphere (Dwiggins, 1975). The standard deviation of each reflexion was estimated from (Toriumi, Ozima, Akaogi & Saito, 1978):

$$[\sigma(|F_o|)]^2 = [\sigma(\text{counting statistics})]^2 + (0{\cdot}014|F_o|)^2. \quad (1)$$

Refinement

The crystal structure had previously been determined by Zachariasen & Ziegler (1931). Further refinement of the structure was carried out with the full-matrix least-squares program *RADIEL* (P. J. Becker, Y. W. Yang and P. Coppens, unpublished). In the least-squares calculation the weight for each reflexion was taken as $w = [\sigma(|F_o|)]^{-2}$, where $\sigma(|F_o|)$ is defined by equation (1). The valence-electron populations, the valence form factors and the extinction parameters were also included in the refinement.

Atomic scattering factors for Cr^{3+}, K^+ and O^- were taken from the values given by Fukamachi (1971), which were chosen as being close to the net charges of the atoms evaluated from the refinement of valence-electron populations. The valence electrons whose populations and form factors were refined were chosen for each atom as follows: Cr^{3+} 3*d*, O^- 2*p*, K^+ 2*p*. The anomalous-scattering factors for Cr, K and O atoms were taken from *International Tables for X-ray Crystallography* (1974).

The intensities of some strong low-angle reflexions were found to change significantly when the intensity variation with azimuthal angle Ψ was measured. This observation could not be accounted for by the absorption effect in view of the spherical shape of the specimen. Thus, type I anisotropic secondary extinction was assumed (Coppens & Hamilton, 1970).

The positional and thermal parameters of the atoms and a scale factor were obtained from 2443 reflexions with $\sin\theta/\lambda \geq 0{\cdot}6$ Å^{-1}. The valence-electron populations and valence form factors were refined on the basis of all the observed reflexions. However, the anisotropic extinction parameters were calculated by using data set 2.

The final positional parameters are listed in Table 2. The valence-electron populations, the valence form factors and the extinction parameters are given in Table 3. The final discrepancy indices are: $R(F) = 0{\cdot}0305$, $R_w(F) = 0{\cdot}0329$ and $S = [\sum w(|F_o| - |F_c|)^2/(n-p)]^{1/2} = 1{\cdot}127$.*

Results and discussion

Description of the structure and discussion

The crystal structure is isotypic with that of K_2SO_4. The crystal is ionic, comprising CrO_4^{2-} and K^+ ions. The bond distances and angles in the CrO_4^{2-} ion are listed in Table 4. The geometry of the CrO_4^{2-} ion is very close to a regular tetrahedron. The average Cr—O bond length is 1·646 (1) Å – slightly longer than the Mn—O bond length of 1·605 Å in the isoelectronic ion

* Lists of structure factors and anisotropic thermal parameters have been deposited with the British Library Lending Division as Supplementary Publication No. SUP 33655 (30 pp.). Copies may be obtained through The Executive Secretary, International Union of Crystallography, 5 Abbey Square, Chester CH1 2HU, England.

Table 2. *Final positional parameters* (×10⁵)

	x	*y*	*z*
Cr	22911 (2)	25000	42061 (2)
K(1)	66568 (5)	25000	41434 (5)
K(2)	−1099 (4)	25000	69989 (3)
O(1)	1549 (18)	25000	42001 (25)
O(2)	30187 (25)	25000	57044 (14)
O(3)	30294 (23)	47750 (21)	34716 (16)

Table 3. *Final values of other parameters*

	Number of valence electrons	Valence form factor κ [defined by $f(s/\kappa)$]
Cr	3·22 (6)	1·136 (10)
K(1)	5·82 (8)	1·109 (6)
K(2)	5·66 (6)	
O(1)	5·40 (4)	1·022 (6)
O(2)	5·32 (6)	
O(3)	5·30 (4)	

Type I anisotropic-extinction parameters (×10⁻⁸)

G_{11}	0·17 (1)	G_{12}	0·09 (3)
G_{22}	0·28 (3)	G_{13}	0·05 (2)
G_{33}	0·27 (2)	G_{23}	0·02 (2)

Scale factor = 3·917 (9).

Table 4. *Bond lengths* (Å) *and angles* (°) *within the* CrO_4^{2-} *ion with their e.s.d.'s in parentheses*

Cr–O(1)	1·637 (1)	O(1)–Cr–O(2)	109·92 (7)
Cr–O(2)	1·654 (2)	O(1)–Cr–O(3)	109·97 (7)
Cr–O(3)	1·648 (1)	O(2)–Cr–O(3)	108·68 (7)
		O(3)–Cr–O(3′)	109·59 (7)

Table 5. *Interatomic distances* (Å) *with their e.s.d.'s in parentheses*

Symmetry code

(i) x, y, z	(v) $0{\cdot}5+x, 0{\cdot}5-y, 1{\cdot}5-z$
(ii) $-1{\cdot}0+x, y, z$	(vi) $-0{\cdot}5+x, 0{\cdot}5-y, 0{\cdot}5-z$
(iii) $-x, 0{\cdot}5+y, 1{\cdot}0-z$	(vii) $0{\cdot}5-x, 1{\cdot}0-y, -0{\cdot}5+z$
(iv) $1{\cdot}0-x, 0{\cdot}5+y, 1{\cdot}0-z$	

Cr···K(1^{i})	3·3457 (6)	Cr···K(2^{i})	3·4359 (5)
Cr···K(1^{iv})	3·5142 (5)	Cr···K(2^{iii})	3·6220 (5)
O(1)···K(1^{ii})	2·681 (2)	O(3)···K(2^{vii})	2·736 (2)
O(1)···K(2^{i})	2·915 (3)	O(3)···K(2^{iii})	2·801 (2)
O(1)···K(2^{iii})	3·211 (1)*	O(3)···K(1^{iv})	2·967 (2)
O(1)···K(1^{vi})	3·660 (3)	O(3)···K(1^{i})	3·166 (2)
O(2)···K(2^{i})	2·749 (2)	O(3)···K(1^{vi})	3·210 (2)
O(2)···K(2^{v})	2·784 (2)		
O(2)···K(1^{iv})	2·974 (1)*		
O(2)···K(1^{i})	3·225 (2)		

* There is an equivalent close contact related by a mirror plane perpendicular to **b**.

MnO_4^- (Palenik, 1967). The interatomic distances are given in Table 5. O atoms are surrounded by five K^+ ions in an approximate square pyramid, and the K···O interatomic distances are in the range 2·681 (2)–3·660 (3) Å.

Thermal motion of the CrO_4^{2-} *ion*

The thermal motion of the CrO_4^{2-} ion was analysed in terms of the rigid-body modes of translation (**T**) and libration (**ω**) (Cruickshank, 1956). The coordinates of the centre of vibration were fixed at the position of the Cr atom. The results are shown in Table 6. The agreement between the observed and calculated thermal parameters, Δ, indicates the rigidity of the CrO_4^{2-} ion. The r.m.s. amplitudes of librational motion are in the range of 5–7°; these are larger than those of translational motion (0·11 Å).

Numbers of electrons around the atoms

The number of electrons in a sphere of radius R with its centre at $\mathbf{r}_i$ was calculated from (Sakurai, 1967):

$$C(R) = \int \rho(r)\,\mathrm{d}v = \frac{1}{V}\left\{\tfrac{4}{3}\pi R^3 F(000) + \frac{1}{2\pi^2}\sum\sum\sum \frac{1}{s^3} \times F(hkl)\exp\left[-2\pi i(\mathbf{s}.\mathbf{r}_i)\right] \times \left[-2\pi sR\cos(2\pi sR) + \sin(2\pi sR)\right]\right\} \quad (2)$$

Table 6. *Rigid-body thermal parameters: magnitudes and directions of the principal components of the molecular translation and libration tensors* (**T** *and* **ω**)

	R.m.s. amplitudes	Components of the principal axes with respect to the crystal axes (×10⁴)		
$T(1)$	0·100 Å	1304	0	43
$T(2)$	0·116	0	1690	0
$T(3)$	0·118	−59	0	961
$\omega(1)$	5·00°	1132	0	479
$\omega(2)$	5·03	0	1690	0
$\omega(3)$	6·94	−650	0	835

$\Delta = \sum_{\text{atom}} \sum_{ij} w(U_{ij}^{\text{obs}} - U_{ij}^{\text{calc}})^2 = 0{\cdot}16 \times 10^{-2}$ (w = atomic weight).

where **s** is a scattering vector, and $s = |\mathbf{s}|$. The radial distribution of electron density around a point $\mathbf{r}_i$ is easily derived by differentiating equation (2) with respect to R:

$$D(R) = \mathrm{d}C(R)/\mathrm{d}R. \quad (3)$$

Errors in $C(R)$ and $D(R)$ were estimated in a similar manner to that utilized in the estimation of $\sigma(\rho)$ (Coppens & Hamilton, 1968; Stevens & Coppens, 1976). Unobserved structure amplitudes have to be included in the calculation of $C(R)$ and $D(R)$:

$$C(R) = \frac{1}{k}C_{\text{obs}}(R) + C_{\text{unobs}}(R). \quad (4)$$

If the errors in the observed structure amplitudes, a scale factor for $C_{\text{obs}}(R)$, and the errors in the refined parameters for $C_{\text{unobs}}(R)$ are taken into account, the variance of $C(R)$ is evaluated as follows:

$$\sigma^2[C(R)] = \frac{1}{k^2}\sigma^2[C_{\text{obs}}(R)] + \left[\frac{\sigma^2(k)}{k^2}\right]\left[\frac{C_{\text{obs}}(R)}{k}\right]^2 + \sum_i \left[\frac{\partial C_{\text{unobs}}(R)}{\partial p_i}\right]^2 \sigma^2(p_i). \quad (5)$$

The first term in equation (5) has been discussed by Coppens & Hamilton (1968), and the explicit form of the third term is

$$\frac{1}{4\pi^4 V^2}\sum_i \left\{\sum_{\text{unobs}} \frac{1}{s^3}\frac{\partial F_h}{\partial p_i}\cos(2\pi s.\mathbf{r}_i)\left[-2\pi sR\cos(2\pi sR) + \sin(2\pi sR)\right]\right\}^2 \sigma^2(p_i). \quad (6)$$

The variance of $D(R)$ was evaluated in a similar way to that of $\sigma^2[C(R)]$.

The number of valence electrons in a sphere of radius R with its centre at $\mathbf{r}_i$ is given by

$$C^v(R) = C^t(R) - C^k(R) \quad (7)$$

where $C^t(R)$ and $C^k(R)$ are the numbers of total and core electrons respectively. $C^k(R)$ was obtained by

direct integration of the calculated electron density given as a Fourier series with the hypothetical structure factors as coefficients; the scattering factor of each atom was replaced by that of the core electrons, leaving the atomic arrangement unchanged. In this case, the errors of $C^k(R)$ should be included in the evaluation of $\sigma^2[C^v(R)]$:

$$\sigma^2[C^v(R)] = \sigma^2[C^t(R)] + \sigma^2[C^k(R)] \qquad (8)$$

where $\sigma^2[C^t(R)]$ is given in equation (5). $\sigma^2[C^k(R)]$ is calculated by equation (6), replacing F_h by the calculated structure amplitudes of the core electrons for the observed reflexions.

Estimated values of $\sigma[C(R)]$ and $\sigma[D(R)]$ for the total and valence electrons are shown in Table 7. In the estimation of $\sigma^2[C(R)]$ and $\sigma^2[D(R)]$, variances of parameters calculated by the least-squares refinement were used, covariances of parameters being neglected. 5753 reflexions with $\sin\theta/\lambda \leq 1{\cdot}407$ Å^{-1} ($2\theta_{\mathrm{Mo}K\alpha} \leq 180°$), including 2863 unobserved reflexions, were used in the calculations. Further corrections for series-termination effects ($\sin\theta/\lambda > 1{\cdot}407$ Å^{-1}) were also made by the method previously described by Kobayashi, Marumo & Saito (1972), using the atomic scattering factors expressed as a sum of Gaussian terms (*International Tables for X-ray Crystallography*, 1974).

As shown in Table 7, the contributions to $\sigma[C(R)]$ and $\sigma[D(R)]$ from the errors in the observed structure amplitudes and the error in a scale factor are large in a sphere (around an atom) of comparatively large radius, in contrast to those from the errors in parameters which are large in a sphere of small radius. It should be remembered that the error in a scale factor may be underestimated by the least-squares calculation (Stevens & Coppens, 1975).

$C(R)$ and $D(R)$ of the valence electrons are easily calculated solely on the basis of the observed structure amplitudes; in other words, they are not affected by the series-termination errors. They contain however, the errors introduced on subtracting the core electrons, the errors due to equivocal selection of the core electrons and the errors in the refined parameters. The latter values are relatively small as shown in Table 7, and the former, though difficult to estimate, may be small. On the other hand, $C(R)$ and $D(R)$ of the total electrons should be corrected for the large series-termination effects, as listed in Table 7. Thus, $C(R)$ and $D(R)$ of the valence electrons may be accurate and useful for the evaluation of the effective atomic charges and for the study of the migration of outer electrons (Coppens, 1975).

The calculated values of $D(R)$ around the Cr and K atoms are shown in Figs. 1 and 2 respectively. The

Table 7. *Contributions to* $\sigma[C(R)]$ *and* $\sigma[D(R)]$ *from the errors in the observed structure amplitudes* (I), *a scale factor* (II) *and the refined parameters* (III) (e Å^{-3})

(I), (II) and (III) correspond to the first, second and third terms in equation (5) respectively. The radii of the spheres in the calculations are: Cr 1·0, K(2) 1·5, O(1) 0·7 Å. The maximum values of the series-termination corrections are shown in parentheses.

Contributions to $\sigma[C(R)]$ of the total electrons

	$C(R)$	$\sigma[C(R)]$	(I)	(II)	(III)	Series-termination correction
Cr	21·74	0·083	0·068	0·048	0·002	−0·395 (0·41)
K(2)	18·04	0·109	0·101	0·040	0·002	0·089 (0·10)
O(1)	5·71	0·037	0·035	0·013	0·002	−0·002 (0·004)

Contributions to $\sigma[C(R)]$ of the valence electrons

	$C(R)$	$\sigma[C(R)]$	(I)	(II)	(III)
Cr	3·94	0·069	0·068	0·009	0·009
K(2)	5·97	0·103	0·101	0·013	0·006
O(1)	2·56	0·039	0·035	0·005	0·016

Contributions to $\sigma[D(R)]$ of the total electrons

	$D(R)$	$\sigma[D(R)]$	(I)	(II)	(III)	Series-termination correction
Cr	6·86	0·213	0·208	0·035	0·041	1·238 (7·35)
K(2)	1·73	0·252	0·252	0·002	0·008	0·692 (1·65)
O(1)	7·71	0·141	0·140	0·018	0·013	0·032 (0·06)

Contributions to $\sigma[D(R)]$ of the valence electrons

	$D(R)$	$\sigma[D(R)]$	(I)	(II)	(III)
Cr	5·70	0·212	0·208	0·012	0·043
K(2)	1·31	0·253	0·252	0·002	0·021
O(1)	5·45	0·141	0·139	0·012	0·017

numbers of valence electrons around the atoms are given in Table 8, with their estimated standard deviations.

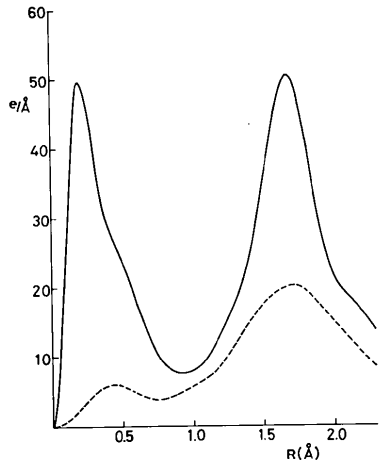

Fig. 1. Radial distribution of the electron density around the Cr atom. Observed values for total electrons (——) and valence electrons (– – – –).

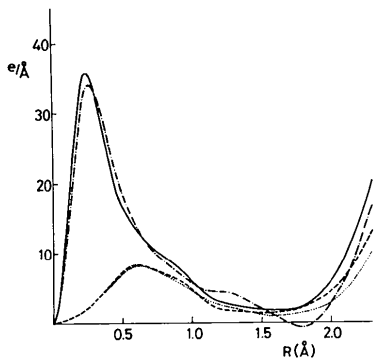

Fig. 2. Radial distributions of the electron densities around the K atoms. Observed values for total electrons (–·–·–) and valence electrons (·····) around the K(1) atom, and observed values for total electrons (——) and valence electrons (– – – –) around the K(2) atom.

In Fig. 2, the radial distributions of valence and total electrons around the K atoms are compared. The radial distribution of the total electrons around K(1) becomes negative in the range of R = 1·6–2·1 Å, possibly owing to the series-termination errors.

Effective charges of the atoms

By allocating an appropriate region for each atom, the effective charges of the atoms were evaluated qualitatively. As shown in Fig. 2, the radial distributions of the valence electrons around the K atoms become minima at distances of 1·60 Å for K(1) and 1·52 Å for K(2) respectively. Accordingly, it may be reasonable to regard the effective regions of the K atoms as spheres of radii equal to these distances, being consistent with the ionic radii of the K^+ ion in crystals (1·52–1·65 Å) (*International Tables for X-ray Crystallography*, 1967). On the other hand, the radial distribution of valence electrons around the Cr atom in Fig. 1 seems to show no apparent radius for the Cr sphere; this is because of the marked superposition of the valence-electron densities of the Cr and four O atoms. The deformation-density map shown in Fig. 4 was averaged on the assumption of T_d symmetry for CrO_4^{2-}. The positive peak attributable to the bonding electrons of the Cr–O bond is located 0·97 Å from the Cr nucleus. This distance agrees with the covalent-bond radius of the Cr atom expected from the bond order of 1·5 for the Cr–O bonds. The covalent radii of O atoms are 0·74 Å for a single bond (O_2 gas) and 0·62 Å for a double bond (O_2^-) respectively (*International Tables for X-ray Crystallography*, 1967). From these data, the covalent radius of 0·97 Å for Cr can be easily evaluated by subtracting the covalent-bond radius of 0·68 Å for the O atom of bond order 1·5 from the mean Cr–O bond length of 1·65 Å. In addition, the curve of the radial distribution of valence electrons around the Cr atom seems to indicate the validity of this covalent radius for the Cr atom. The spherical region of each atom is illustrated in Fig. 3. The electron density in the crystal can be expressed as a sum of the

Table 8. *The numbers of valence electrons in the spheres of radius R around the atoms, with their e.s.d.'s in parentheses*

	Cr		K(1)	K(2)		O(1)	O(2)	O(3)
R	$C(R)$	R	$C(R)$	$C(R)$	R	$C(R)$	$C(R)$	$C(R)$
0·70 Å	2·62 (4)	1·10 Å	5·17 (8)	5·27 (8)	0·40 Å	0·86 (2)	0·90 (2)	0·87 (1)
0·75	2·81 (4)	1·20	5·45 (9)	5·50 (9)	0·50	1·41 (2)	1·47 (2)	1·43 (2)
0·80	3·00 (5)	1·30	5·67 (10)	5·67 (9)	0·55	1·70 (3)	1·77 (3)	1·72 (2)
0·85	3·21 (5)	1·40	5·84 (11)	5·83 (10)	0·60	1·99 (3)	2·07 (3)	2·01 (2)
0·90	3·43 (6)	1·50	5·97 (11)	5·97 (10)	0·65	2·28 (4)	2·37 (4)	2·30 (3)
0·95	3·67 (6)	1·55	6·01 (11)	6·03 (10)	0·70	2·56 (4)	2·65 (4)	2·57 (3)
1·00	3·94 (7)	1·60	6·06 (12)	6·10 (11)	0·75	2·82 (4)	2·91 (4)	2·84 (3)
1·05	4·24 (7)	1·70	6·15 (12)	6·26 (11)	0·80	3·07 (5)	3·17 (5)	3·09 (3)
1·10	4·57 (8)	1·80	6·27 (12)	6·46 (11)	0·85	3·31 (5)	3·41 (5)	3·33 (3)
1·15	4·94 (9)	1·90	6·43 (12)	6·73 (11)	0·95	3·73 (6)	3·86 (6)	3·77 (4)

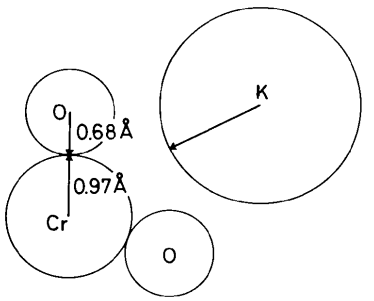

Fig. 3. Spherical region of each atom.

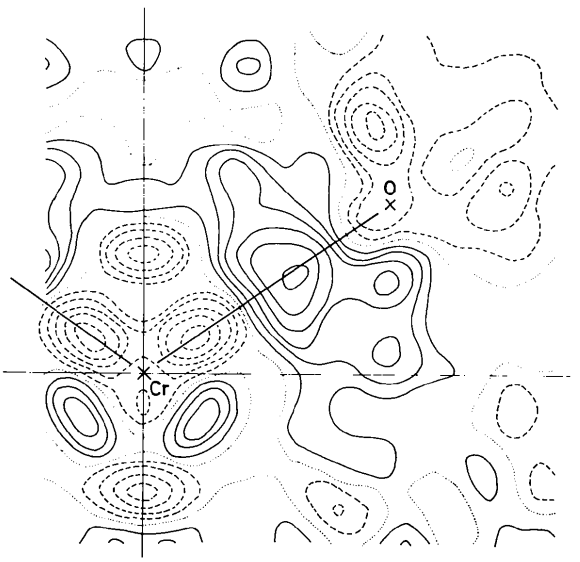

Fig. 4. Average deformation density in the plane containing a Cr and two O atoms. Contours are at intervals of 0·05 e Å^{-3}. Zero contours are in dotted lines, and negative contours broken.

electrons in each spherical region of atoms and those in the interatomic region.

The results of the direct integration of electron densities are summarized in Table 9, together with the net charges of the atoms obtained by the refinement of the valence-electron populations. There arises the question of how to allocate the electrons in the interatomic region to each atom. By making a very rough assumption that one fifth of the electrons in the interatomic region belong to each Cr and O atom, the effective charge of each atom can be evaluated. The results are listed in Table 9.

On these assumptions, the effective charges of the Cr, O and K atoms were estimated as +0·1, −0·5 and +1·0 e respectively. If only those valence electrons located in a sphere of radius 0·97 Å around the Cr atom are considered to belong to the Cr atom, the effective charge of the Cr atom becomes +2·2 e. The largely neutralized charges of Cr and O atoms, relative to the extreme ionic limits of +6 and −2 for Cr and O atoms on the basis of formal valence theory, may not be surprising and it may be concluded that the 3*d* atomic orbitals of the Cr atom contribute significantly to the Cr—O bonding orbitals. It should be noted that the effective charges of the Cr and O atoms estimated as above are significantly different from those given by the analysis of valence-electron populations. This disagreement may be due to a marked change in valence-electron distribution on multiple-bond formation.

Residual electron-density distribution

A three-dimensional difference Fourier map was calculated with 2826 reflexions for which the calculated structure amplitudes were greater than 2·0. 64 reflexions with $|F_o| < 2{\cdot}0$ were excluded from the calculation

Table 9. *Effective charges* (e) *of the atoms*

		Number of electrons within a sphere of radius *R*		Effective charges of the atoms	
	R	(I)*	(II)†	Estimated from (II)	Refinement of valence-electron populations
K(1)	1·60 Å	18·37 (12)	17·99 (10)		+1·18 (8)
K(2)	1·52	18·07 (11)	18·06 (12)		+1·34 (6)
Average		18·22	18·03	+0·97 (8)‡	
Cr	0·97	21·49 (8)	21·83 (7)	+0·13 (11)	+2·78 (6)
O(1)	0·68	5·55 (4)	6·45 (4)		−1·40 (4)
O(2)	0·68	5·66 (4)	6·53 (4)		−1·32 (6)
O(3)	0·68	5·55 (2)	6·46 (3)		−1·30 (4)
Average		5·59	6·48	−0·48 (8)	
Interatomic region		13·76 (19)	10·22 (18)		

* Total number of electrons obtained by the direct integration.
† Sum of core electrons and the integrated valence density.
‡ Only the errors in charge integration are considered in estimating the errors of the atomic charges.

because of the uncertainty in their phases. There are four crystallographically independent and chemically equivalent segments containing a Cr and two O atoms. Any remarkable common features could not be discerned, since each difference map contained a number of spurious peaks. Accordingly, the weighted average map was calculated in order to detect any remarkable common features. The result is shown in Fig. 4. The procedure for obtaining the weighted average of the electron density was described by Rees (1976), neglecting the correlations between two points. The estimated standard deviation of the averaged deformation density, $\sigma(\overline{\Delta\rho})$, in the same section is also shown in Fig. 5. The contributions to $\sigma(\Delta\rho)$ from the errors in a scale factor and the observed structure amplitudes are considered, but the errors in the refined parameters are neglected. The errors in the observed structure amplitudes are estimated from (Stevens & Coppens, 1976):

$$\sigma'(|F_o|)^2 = \sigma(|F_o|)^2/n \qquad (9)$$

where $\sigma(|F_o|)^2$ is given by equation (1), and n is the number of observed symmetry-related reflexions.

A remarkable feature in Fig. 4 is the distribution of the residual peaks around the Cr atom. A positive peak (with peak height 0·2 e Å^{-3}) is 0·40 Å from the Cr nucleus on the extension of the O—Cr bond. However, a negative peak (0·30 e Å^{-3}) is located 0·35 Å from the Cr nucleus on the Cr—O bond. In the three-dimensional maps, four positive and four negative peaks are arranged (alternately) at the eight corners of a cube centred at the Cr nucleus. These peaks may be significant since their peak heights are greater than three times the estimated standard deviations of the electron densities at the corresponding points.

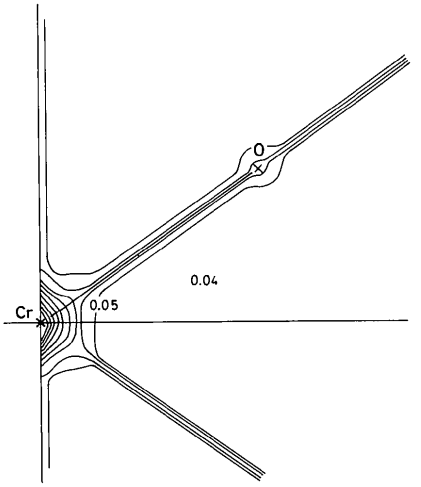

Fig. 5. Error distribution in average deformation density in the same plane as Fig. 4. Contours are at intervals of 0·02 e Å^{-3}. The minimum value is 0·04 e Å^{-3}.

Let us consider the 3*d* atomic orbitals of a Cr atom. The geometry of the CrO_4^{2-} ion possesses T_d symmetry. Accordingly, the 3*d* atomic orbitals of a Cr atom split into *e* ($d_{x^2-y^2}$, d_{z^2}) and t_2 orbitals (d_{xy}, d_{xz}, d_{yz}). There are significant contributions by these atomic orbitals to the Cr—O bonding orbitals, as mentioned above. The lobes of the t_2 orbitals which have σ-bonding character are directed along the threefold axes of the tetrahedron, and those of the *e* orbitals which have π-bonding character are directed along the diad.

Johansen (1976) has calculated the theoretical deformation density for the MnO_4^- ion by using the *ab initio* Hartree–Fock configuration-interaction method. Since the CrO_4^{2-} ion is isoelectronic with the MnO_4^- ion, it may be reasonable to compare the electron-density distribution in CrO_4^{2-} with that in MnO_4^-. The theoretical deformation density is slightly different from that observed, probably owing to the neglect of thermal vibration and the Coulombic effects of the neighbouring ions. The theoretical deformation map (Fig. 3 of Johansen, 1976) shows pronounced positive peaks around the Mn nucleus. These are at 0·30 Å from the Mn nucleus on the extension of the O—Mn bond (the peak height being about 2 e Å^{-3}). The theoretical deformation density around the Mn atom almost agrees with that observed around the Cr atom. Johansen claims that these peaks arise from excess charge in the t_2 orbitals and deficiency in the *e* orbitals. The same result was reported by Johnson & Smith (1972), who calculated the electron-density distribution in the MnO_4^- ion by the SCF–$X\alpha$–SW method. The experimental result also indicates that the contribution of the 3*d* atomic orbitals of a Cr atom to the t_2 molecular orbitals is larger than that to the *e* molecular orbitals.

The positive peak due to the bonding electrons of the Cr—O bond appear at 0·97 Å from the Cr nucleus with a peak height of 0·30 e Å^{-3}. This peak is elongated perpendicular to the Cr—O bond. This may indicate the double-bond character of the Cr—O bond, but there is also smearing because of the librational motion of the CrO_4^{2-} ion.

The calculations were carried out on the FACOM 230-48 computer of this Institute and the HITAC 8800/8700 computer at the Computer Centre of the University of Tokyo. Part of the cost of this research was met by a Scientific Research Grant from the Ministry of Education, to which the authors' thanks are due.

References

COPPENS, P. (1975). *Phys. Rev. Lett.* **35**, 98–100.

COPPENS, P. & HAMILTON, W. C. (1968). *Acta Cryst.* B**24**, 925–929.

COPPENS, P. & HAMILTON, W. C. (1970). *Acta Cryst.* A**26**, 71–83.

CRUICKSHANK, D. W. J. (1956). *Acta Cryst.* **9**, 754–756.

DWIGGINS, C. W. JR (1975). *Acta Cryst.* A**31**, 395–396.
FUKAMACHI, T. (1971). Tech. Rep. B12. Institute for Solid State Physics, Univ. of Tokyo.
International Tables for X-ray Crystallography (1967). Vol. II, 2nd ed. Birmingham: Kynoch Press.
International Tables for X-ray Crystallography (1974). Vol. IV. Birmingham: Kynoch Press.
IWATA, M. (1977). *Acta Cryst.* B**33**, 59–69.
IWATA, M. & SAITO, Y. (1973). *Acta Cryst.* B**29**, 822–832.
JOHANSEN, H. (1976). *Acta Cryst.* A**32**, 353–355.
JOHNSON, K. H. & SMITH, F. C. JR (1972). *Phys. Rev. Sect. B*, **5**, 831–843.
KOBAYASHI, A., MARUMO, F. & SAITO, Y. (1972). *Acta Cryst.* B**28**, 2709–2715.
MARUMO, F., ISOBE, M. & AKIMOTO, S. (1977). *Acta Cryst.* B**33**, 713–716.
MARUMO, F., ISOBE, M., SAITO, Y., YAGI, T. & AKIMOTO, S. (1974). *Acta Cryst.* B**30**, 1904–1906.
PALENIK, G. J. (1967). *Inorg. Chem.* **6**, 503–507.
PISTORIUS, C. W. F. T. (1962). *Z. Phys. Chem.* (*Frankfurt am Main*), **35**, 109–121.
REES, B. (1976). *Acta Cryst.* A**32**, 483–488.
SAKURAI, T. (1967). *X-ray Crystal Structure Analysis.* Tokyo: Shokabo.
STEVENS, E. D. & COPPENS, P. (1975). *Acta Cryst.* A**31**, 612–619.
STEVENS, E. D. & COPPENS, P. (1976). *Acta Cryst.* A**32**, 915–917.
TORIUMI, K., OZIMA, M., AKAOGI, M. & SAITO, Y. (1978). *Acta Cryst.* B**34**, 1093–1096.
ZACHARIASEN, W. H. & ZIEGLER, G. E. (1931). *Z. Kristallogr.* **80**, 164–173.

Acta Cryst. (1978). B**34**, 3156–3160

Structure Cristalline d'un Oxotellurate, $Li_4Te^{VI}O_5$, à Groupement Anionique Individualisé: $Te_2^{VI}O_{10}^{8-}$

PAR JACQUES MORET, FRANÇOISE DANIEL, WALOEJO LOEKSMANTO, MAURICE MAURIN ET ETIENNE PHILIPPOT

Laboratoire de Chimie Minérale C, ERA 314, *Chimie des Matériaux, Université des Sciences et Techniques du Languedoc, Place E. Bataillon,* 34060 *Montpellier CEDEX, France*

(*Reçu le* 21 *mars* 1978, *accepté le* 30 *mai* 1978)

Li_4TeO_5 is triclinic, space group $P\bar{1}$, with cell parameters $a = 5{\cdot}186$ (1), $b = 7{\cdot}765$ (1), $c = 5{\cdot}120$ (1) Å, $\alpha = 101{\cdot}96$ (1), $\beta = 101{\cdot}89$ (1), $\gamma = 107{\cdot}58$ (1)° and $Z = 2$. The structure was solved by means of Patterson and Fourier syntheses and refined to a final R value of 0·02. This structure is characterized by a dimeric anion $Te_2O_{10}^{8-}$, made up of two edge-sharing octahedra TeO_6. From this structure, it is apparent that Li_4TeO_5 is of the NaCl type, with the Te and Li atoms distributed over the cation positions. The ordered layers are parallel to the (**a** + **b**, **c**) plane. These are composed of two close-packed planes of O atoms between which the Li and Te atoms occupy $\frac{3}{5}$ and $\frac{2}{5}$ of the octahedral holes, respectively. Between two such sheets, there are Li atoms in all the octahedral holes.

Introduction

Dans le cadre de nos recherches sur les composés oxygénés du tellure afin d'élucider les problèmes de coordination du tellure(IV) et du tellure(VI), nous avons recherché dans les systèmes Li_2O–TeO_2–TeO_3 l'obtention de phases mixtes. C'est ainsi qu'il avait été avancé la présence possible, lors de la dégradation de Li_2TeO_4 pour donner Li_2TeO_3, d'une phase $Li_4Te_2O_7$.

Des monocristaux avaient alors pu être isolés de la masse obtenue par traitement d'un mélange Li_2TeO_4, Li_2TeO_3 comprimé à 12 t cm^{-2} puis porté rapidement à 850 °C et ensuite trempé. Les caractéristiques cristallographiques obtenues à partir d'un de ces monocristaux avaient été présentées comme étant celles de $Li_4Te_2O_7$ (Cachau-Hereillat, 1972; Moret, Norbert & Cachau-Hereillat, 1973).

Nous avons donc entrepris l'étude structurale détaillée de cette phase qui a montré que l'on était en présence d'une phase cristalline de formule globale Li_4TeO_5 mettant en jeu exclusivement le tellure au degré d'oxydation VI et présentant un arrangement anionique inédit.

Sans renoncer à l'hypothèse avancée d'une phase intermédiaire mixte $Li_4Te_2O_7$, il est certain que les conditions d'obtention de celle-ci posent des problèmes qui n'apparaissent pas encore résolus et sur lesquels nous travaillons. Nous nous proposons de présenter ici les résultats de l'étude structurale de Li_4TeO_5.

Données expérimentales

A partir des études préliminaires déjà mentionnées (Cachau-Hereillat, 1972; Moret *et al.*, 1973), nous